Structural, Morphological, and Textural Properties of Coprecipitated $CaTiO_3$ for Anion Exchange in the Electrolyzer

D. Parajuli, N. Murali, K. Samatha, N. L. Shah and B. R. Sharma

Journal of Nepal Physical Society

Volume 9, Issue 1, June 2023

ISSN: 2392-473X (Print), 2738-9537 (Online)

JNPS, **9** (1): 137-142 (2023)

DOI: https://doi.org/10.3126/jnphyssoc.v9i1.57751

Published by:

Nepal Physical Society
P.O. Box: 2934
Tri-Chandra Campus
Kathmandu, Nepal
Email: nps.editor@gmail.com

JNPS 9 (1): 137-142 (2023)
ISSN: 2392-473X (Print), 2738-9537 (Online)

DOI: https://doi.org/10.3126/jnphyssoc.v9i1.57751

Structural, Morphological, and Textural Properties of Coprecipitated $CaTiO_3$ for Anion Exchange in the Electrolyzer

D. Parajuli[1, 2, *], N. Murali[2], K. Samatha[3], N. L. Shah[4] and B. R. Sharma[5]
[1]Research Center for Applied Science and Technology, Tribhuvan University, Nepal
[2]Department of Engineering Physics, AUCE (A), Andhra University, Visakhapatnam, India
[3]Department of Physics, AUCST, Andhra University, Visakhapatnam, India
[4]Department of Physics, Tri-Chandra Multiple Campus, Kathmandu, Nepal
[5]Department of Physics, Janapriya Multiple Campus, Pokhara, Kaski
*Corresponding Email: deepenparaj@gmail.com

Received: *20th May, 2023;* ***Revised:*** *22nd June, 2023;* ***Accepted:*** *30th June, 2023*

ABSTRACT

The limitation in fossil fuel and the emission of greenhouse gases (GHG) resulting in global warming is one of the global challenging issues. Similarly, efficient and cost-effective renewable energy resources are always in demand for the overcome of the limitation. One of the best alternatives to fossil fuels based on renewable energy sources is hydrogen fuel. The main component of the hydrogen fuel generator is the Electrolyzer. Among different types of electrolyzers, the incorporation of an anion exchange membrane is one approach. In this work, we are focusing on the preparation, characterization, and analysis of anion exchange material CaTiO3 used for the electrolyzer. A co-precipitation method was used for the preparation of CaTiO3 XRD shows the orthorhombic structure of the CaTiO3. FT-IR shows the vibrational spectra of CaTiO3. The particles were spherical and crystalline with an average size of 200 nm when viewed through the Scanning Electron Microscope (SEM), Transmission Electron Microscopy (TEM), and High-Resolution Transmission Electron Microscopy (HRTEM). The SAED pattern verifies the single crystalline nature of the sample. In this way, the CaTiO3, the anion exchange agent was synthesized and characterized successfully.

Keywords: Coprecipitation, Oxalate hydroxide, Anion exchange, Electrolyzer, Calcium titanate.

I. INTRODUCTION

Currently, Currently, researchers in the field of material science are interested in synthesizing various nanosized materials [1]. We are focusing our research on energy (Solar [1–3], MXenes [4–6], Ferrites [7, 8], etc.) energy storage [9,10] and energy-efficient device production with several manufacturing approaches. Ceramic materials are one of them with their different types. Among different types of ceramics, Perovskite [11] belongs to a novel class of material with a variety of potential technological applications [12,13]. ABX3 is the format of Perovskite with larger divalent and smaller tetravalent cations A and B respectively that are bound with anion X (like O^{-2}) as shown in Figure 1. Calcium Titanate (CaTiO3) can have cubic, tetragonal, and orthorhombic structures [14] with higher dielectric properties that are used in wireless communication systems as resonators [15,16]. Wang et al. found Ti- electrodes coated with CaTiO3 that are highly resistant to corrosion. Higher catalytic efficiency for the production of hydrogen through electrolysis is shown by CaTiO3 doped with Platinum, Zr4+, CoO, etc. [12,17]. Since calcium titanate-based ceramics form a number of solid solutions with lanthanides and actinides, they find applications in the storage and treatment of nuclear wastes [18,19]. In medicine, calcium titanate is highly useful due to its bio-compatibility and finds applications in fabricating materials for bone and joint repair [12,20]. Titanium alloys are widely used as metallic

implantable materials and calcium titanate coating is an effective method to enhance biocompatibility [21] of titanium surfaces [22].

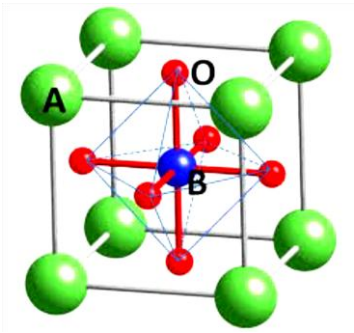

Fig. 1: Chemical structure of Perovskite.

CaTiO3 can be used for the production of Calcium titanate hydroxide (HCaTiO3OH), an efficient anion-exchange material [23]. The exchange of anions is attained when CaTiO3 is mixed with base NaOH as shown in the following equation:

$$CaTiO3+2NaOH+CaCl_2 \rightarrow HCaTiO3OH+2NaCl \quad \ldots\ldots(1)$$

There are various methods for the preparation of nano-sized calcium titanate particles, including solid-state [24, 25], sol-gel [26, 27], hydrothermal [25], co-precipitation [28], mechanical alloying [29], Solvothermal methods [30,31], etc. The co-precipitation method is widely used to synthesize ceramic materials since this method is simple and the mixing of the reagents occurs on an atomic level rather than a particulate level. Y.K. Sharma et al. used coprecipitation methods mixed metal oxalates for the synthesis of transition metal titanates (MTiO3), (M = Mn, Fe, Co, Ni, and Cd) by adding transition metal chlorides to potassium titanyl oxalate solution [32]. The X-ray Diffractometer (XRD) pattern showed that the MTiO3 was not phase pure and contained significant amounts of transition metal oxides and other impurities [31].

Here, we report the synthesis of calcium titanate nanopowder by a novel coprecipitation method in the ammoniacal medium using a simple precursor potassium titanyl oxalate followed by calcination. The structure and morphology of the synthesized nanopowder were studied by X-ray Diffractometer (XRD), Fourier Transform Infrared (FTIR) spectroscopy, High-Resolution Transmission Electron Microscopy (HRTEM), Scanning Electron Microscope (SEM), and Energy Dispersive X-ray (EDX) Spectroscopy techniques.

II. Experimental

Synthesis of CaTiO3

20 g potassium titanyl oxalate ($C_4K_2O_9Ti$) (Sigma Aldrich) and 6 g calcium chloride ($CaCl_2$) (Sigma Aldrich) were mixed with 250 ml Double Ionized (DI) water which is then mixed slowly with 250 ml 0.2M ammonium oxalate solution ($NH_4C_2O_4$) in ammonium hydroxide to get [CaTi(OH)x(C2O4)y]. The solution was maintained at a pH of 9 by adding 25% ammonia solution and stirring for 2 h on a magnetic stirrer. The resulting white slurry was kept overnight for aging at room temperature. It was then filtered, washed with DI water, and dried at 80°C for two days. The dried precipitate was ground to a fine powder and was calcined at 900°C for 2 h to obtain pure calcium titanate.

The synthesis procedure of CaTiO3 is shown in equation (2).

$$K_2[TiO(C_2O_4)_2].2H_2O \xrightarrow{(NH_4)C_2O_4.NH_4OH} CaTi(OH)_x(C_2O_4)_y \xrightarrow{900^oC,2h} CaTiO_3 \quad \ldots\ldots\ldots\ldots\ldots\ldots\ldots\ldots(2)$$

Characterization Techniques

SHIMADZU, XRD700 powder diffractometer at room temperature incorporating Co-Kα radiation was used for the determination of the structural parameter of the sample under consideration. The range of the scan was 20-80° (2θ) in 0.0196° (2θ) step. Similarly, the range of 400-4000 cm-1 was used for the FT-IR spectrum using the L160000A Perkin Elmer instrument. Calcium titanate was treated with 2M NaOH for 24 h at room temperature (RT) for a hydroxylation reaction. It was washed with water, then dried, and recorded their FT-IR spectra. JEOL 4000EX High-Resolution Transmission Electron Microscope (HRTEM) operated at 400 kV was used for transmitted images. Ion sputtering of gold was done over the samples JSM-5600, JEOL Co., Japan was used for SEM images followed with EDS.

III. RESULTS AND DISCUSSION

XRD analysis

The XRD pattern of CaTiO3 obtained after calcination at 900°C of CaTi(OH)x(C2O4)y is

shown in Fig.2. The peaks were obtained at 32.7°, 47.1 °, 58.9 °, and 69 ° corresponding to the hkl values (121), (202), (123), (242) [15, 19] that matched well with Joint Committee on Powder Diffraction Standards (JCPDS) No. 22-153 [33, 34]. The crystal structure shows pure orthorhombic perovskite (CaTiO3) powder. The crystallite size of the material was calculated using the Debye-Scherrer formula [35] as given in equation (3).

$$d = \frac{0.9\lambda}{\beta cos\theta} \quad \text{.....(2)}$$

Where d is the crystallite size, λ is the X-ray wavelength, β is the full width at half maxima and θ is the Bragg's angle. From this equation, the synthesized material's average crystallite size was approximately 200 nm.

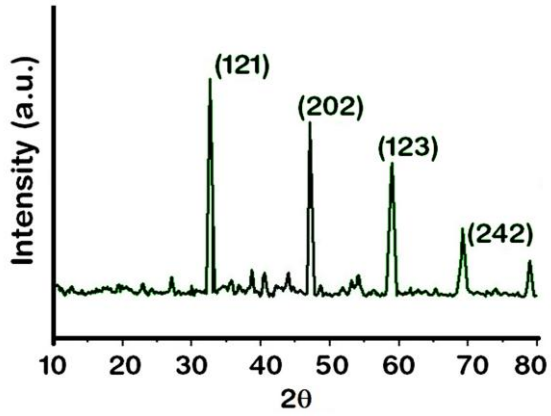

Fig. 2: XRD pattern of $CaTiO_3$ powder.

FTIR analysis

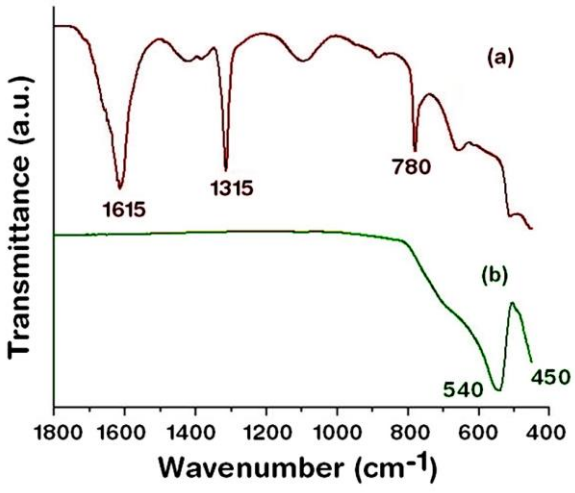

Fig. 3: FT-IR spectrum of mixed oxalate and hydroxide of calcium and Titanium (a) before calcination (b) after calcinations.

FT-IR spectra of the sample before and after calcination of the sample are shown in Fig. 3 (a-b). The peak at 1615 cm^{-1} corresponds to the antisymmetric O-C-O stretching vibrations of the oxalate, 1315 cm^{-1} to symmetric O-C-O stretching vibrations, and 780 cm-1 is related to the in-plane O-C-O deformation vibrations, indicating the presence of oxalate group in the sample [36]. Spectrum in 3(b) shows the absence of characteristic bands of the oxalate group, indicating the complete elimination of oxalate after calcination at 900°C for 2 h. The absorption band at 540 cm^{-1} corresponds to specific stretching vibrations of Ti-O bonds [35, 37] and the band at 450 cm^{-1} is a characteristic feature of Ca-Ti-O bending vibrations of calcium titanate [30]. The absence of characteristic vibrations of oxalate after calcination at 900°C reveals the formation of pure CaTiO3. Similarly, the FT-IR spectrum of calcium titanate before and after hydroxylation is presented in Fig. 4 (a-b). The two peaks in 4(b) at 540 cm^{-1} and 450 cm^{-1} in the spectrum of CaTiO3 are related to that of Ti-O bonds [35] and Ca-Ti-O bending vibrations [30] respectively. As seen in Fig. 4(b) the 3400-3200 cm^{-1} region is related to stretching vibrations of –OH groups of HCaTiO3OH.

SEM-EDX analysis

Fig. 5 shows the microstructures like grain size, shape, and agglomeration of the $CaTiO_3$ particles with the Scanning Electron Microscope (SEM). The images show the agglomerated composition of spherical particles with a size of 200nm on average. EDX spectrum of calcium titanate shown in Fig. 6 indicates the presence of Ca, Ti, and O atoms in accurate proportion in the prepared material. This further confirmed the formation of pure $CaTiO_3$.

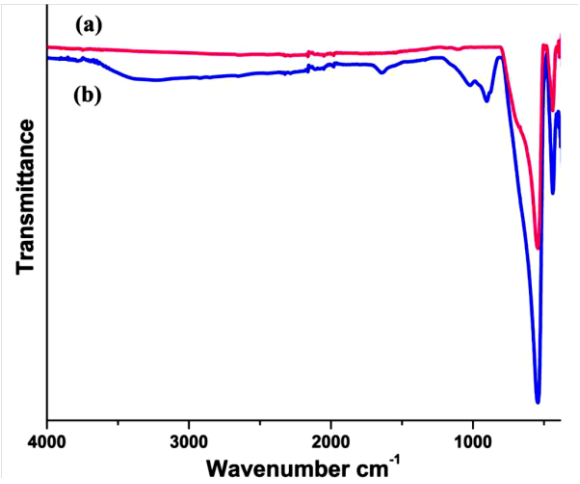

Fig. 4: FT-IR spectrum of calcium titanate (a) before hydroxylation (b) after hydroxylation.

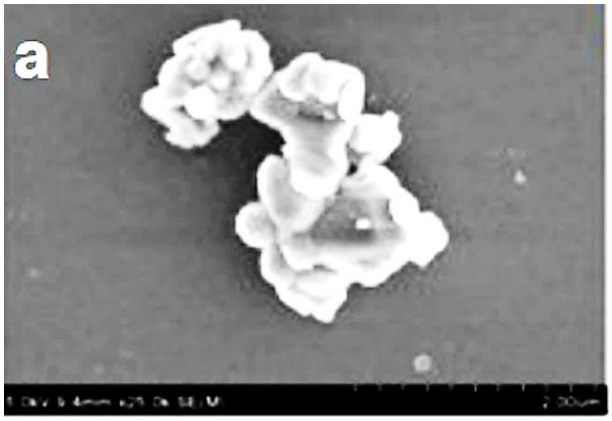

Fig. 5: SEM images of $CaTiO_3$.

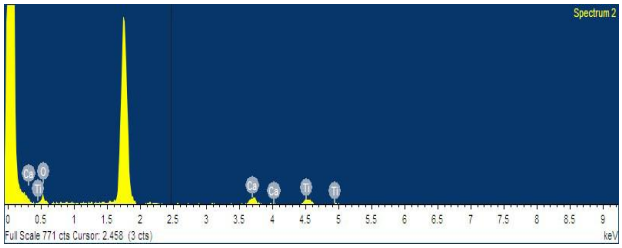

Fig. 6: EDX spectrum of $CaTiO_3$.

TEM analysis

The texture and particle size of $CaTiO_3$ were further observed through TEM, HRTEM, and SAED patterns as shown in Fig. 7 (a, b), (c), and (d) respectively. The nanoparticles in the cluster are seen from TEM images of CaTiO3 powders. The images show the spherical particle with an average size of 200 nm same as that of the SEM image. The interplanar spacing 'd' of 0.32 nm is detected from HRTEM images in Fig. 7 (c). The crystal planes in the form of dotted rings are obtained from the SAED pattern of $CaTiO_3$ indicating its freestanding single-crystal nature.

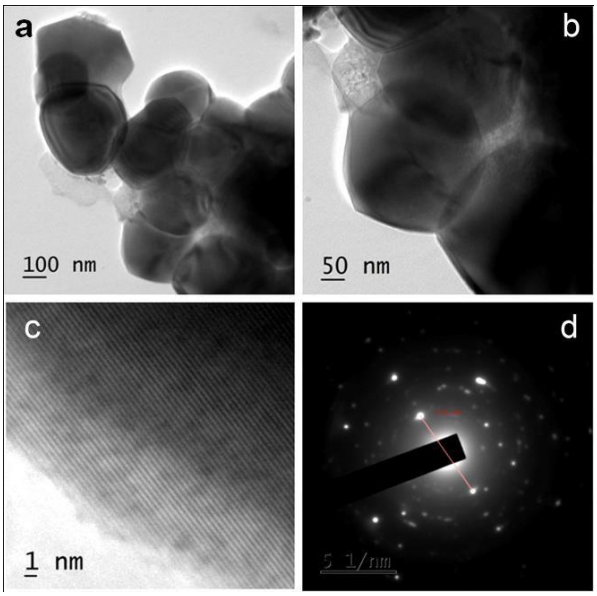

Fig. 7: Images of $CaTiO_3$ with (a, b) TEM at 100 nm and 50 nm (c) HRTEM (d) SAED.

IV. CONCLUSIONS

A co-precipitation method was used for the preparation of $CaTiO_3$ in which $C_4K_2O_9Ti$ and $CaCl_2$ solution in the presence of NH_4OH to form precipitating [CaTi(OH)x(C2O4)y] and then calcinated. The structure of the $CaTiO_3$ is found to be orthorhombic by XRD. FT-IR shows the vibrational spectra of $CaTiO_3$. The particles were spherical and crystalline with an average size of 200 nm when viewed through the SEM, TEM, and HRTEM. The SAED pattern verifies the crystalline nature of the sample. Morphological features investigated with SEM, reveal that the CaTiO3 particles are having a spherical shape with a diameter of approximately 200 nm.

REFERENCES

[1] Demirors, A. F. & Imhof, A. $BaTiO_3$, $SrTiO_3$, $CaTiO_3$, and Ba xSr1-xTiO_3 particles: A general approach for monodisperse colloidal perovskites. *Chemistry of Materials*, **21** (13): 3002–3007 (2009).

[2] Dong, W.; Zhao, G.; Bao, Q. & Gu, X. Solvothermal Preparation of $CaTiO_3$ Prism and CaTi2O4(OH)2 Nanosheet by a Facile Surfactant-Free Method. *Materials Science*, **21** (4): 583–585 (2015).

[3] Dubey, A. K.; Basu, B.; Balani, K.; Guo, R. & Bhalla, A. S. Multifunctionality of Perovskites $BaTiO_3$ and CaTiO3 in a Composite with Hydroxyapatite as Orthopedic Implant Materials. **131** (1): 119–126 (2011).

[4] Hernandez-Sanchez, B. A. & Tuttle, B. A. *Oxalate co-precipitation synthesis of calcium zirconate and calcium titanate powders* (2009).

[5] Mallik, P. K.; Biswal, G.; Patnaik, S. C. & Senapati, S. K. Characterisation of Sol-Gel Synthesis of Phase Pure CaTiO3 Nano Powders after Drying. *IOP Conference Series: Materials Science and Engineering*, **75** (1): 012005 (2015).

[6] Manafi, S. & Jafarian, M. Synthesis of perovskite CaTiO3 nanopowders with different morphologies by mechanical alloying without heat treatment. *International Journal of Physical Sciences* (2013).

[7] Manafi, S. & Jafarian, M. Determining the Optimal Conditions for Calcium Titanate Nanostructures Synthesized by Mechanical Alloying Method. *Advanced Ceramics Progress*, **1** (1): 11–16 (2015).

[8] Mandal, K. An Overview on Recent Developments in the Synthesis, Characterization and Properties of High Dielectric Constant Calcium Copper Titanate Nano-Particles. *Nanoscience & Technology: Open Access*, **1** (2): (2014).

[9] Marques, V. S.; Cavalcante, L. S.; Sczancoski, J. C.; Paris, E. C.; Teixeira, J. M. C. et al. Synthesis of (Ca,Nd)TiO3 powders by complex polymerization, Rietveld refinement and optical properties. *Spectrochimica Acta Part A: Molecular and Biomolecular Spectroscopy*, **74** (5): 1050–1059 (2009).

[10] Moly, P. P.; Jeena, C. B.; Elsa, P. J.; Ambily, K. J. & Joy, V. T. High performance polyvinyl alcohol/calcium titanate nanocomposite anion-exchange membranes as separators in redox flow batteries. *Polymer Bulletin*, **75** (10): 4409–4428 (2018).

[11] Muccillo, R. & Carmo, J. R. Synthesis and Characterization of Strontium and Calcium Titanate Polycrystalline Powders by a Modified Polymeric Precursor Technique. *Materials Science Forum*, 727–728: 904–908 (2012).

[12] Murali, N.; Babu, K. E.; Taddesse, P. S.; Ramakrishna, A.; Parajuli, D. et al. Theoretical investigation of structural, electronic, dielectric and optical characteristics of cubic perovskite BaCeO3. *Processing and Application of Ceramics*, **15** (4): 351–356 (2021).

[13] Nirmala, P. N. & Suresh, G. Synthesis and Characterization of Barium Titanate, Calcium Titanate and Strontium Titanate Thin Films. *International Journal of Scientific & Engineering Research*, **5** (7): 587–594 (2014).

[14] Parajuli, D.; Bhandari, V.; K.C., D.; Thapaliya, A.; Subedi, A. et al. Numerical Approach of Single-Junction InGaN Solar Cell Affected by Carrier Lifetime and Temperature. *Pragya Darshan*, **5** (1): 58–63 (2023).

[15] Parajuli, D.; K.C., D.; Reda, T. G.; Sravani, G. M.; Murali, N. & Samatha, K. RHEED analysis of the oxidized M′2M″xXyene sheets by ablated plasma thrust method in pulsed laser deposition chamber. *AIP Advances*, **11** (11): 115019 (2021).

[16] Parajuli, D.; Kaphle, G. C.; Murali, N. & Samatha, K. Structural Identification of Cubic Aluminum and Non-Cubic Titanium using X-Ray Diffractometer. *Journal of Lumbini Engineering College*, **4** (1): 62–71 (2022).

[17] Parajuli, D.; Murali, N.; K. C, D.; Karki, B.; Samatha, K. et al. Advancements in MXene-Polymer Nanocomposites in Energy Storage and Biomedical Applications. *Polymers 2022*, **14** (16): 3433 (2022).

[18] Parajuli, D.; Murali, N.; Rao, A. V.; Ramakrishna, A. S. Y. M. & Samatha, K. Structural, dc electrical resistivity and magnetic investigation of Mg, Ni, and Zn substituted Co-Cu nano spinel ferrites. *South African Journal of Chemical Engineering*, **42:** 106–114 (2022).

[19] Parajuli, D.; Murali, N.; Samatha, K. & Veeraiah, V. Thermal, structural, morphological, functional group and first cycle charge/discharge study of Co substituted LiNi1−x-0.02Mg0.02CoxO2 (x = 0.00, 0.02, 0.04, 0.06, and 0.08) cathode material for LIBs. *AIP Advances*, **12** (8): 085010 (2022).

[20] Parajuli, D.; Shah, D. K.; K. C., D.; Kumar, S.; Park, M. & Pant, B. Influence of Doping Concentration and Thickness of Regions on the Performance of InGaN Single Junction-Based Solar Cells : A Simulation Approach. *Electrochem*, **3:** 407–415 (2022).

[21] Parajuli, D.; Taddesse, P.; Murali, N. & Samatha, K. Correlation between the structural, magnetic, and dc resistivity properties of Co0.5M0.5-xCuxFe2O4 (M = Mg, and Zn) nano ferrites. *Applied Physics A: Materials Science and Processing*, **128** (1): 1–9 (2022).

[22] Parajuli, D.; Taddesse, P.; Murali, N.; Veeraiah, V. & Samatha, K. Effect of Zn2+ doping on thermal, structural, morphological, functional group, and electrochemical properties of layered LiNi0.8Co0.1Mn0.1O2 cathode material. *AIP Advances*, **12** (12): 125012 (2022).

[23] Parajuli, D.; Uppugalla, S.; Murali, N.; Ramakrishna, A.; Suryanarayana, B. & Samatha, K. Synthesis and characterization MXene-Ferrite nanocomposites and its application for dying and shielding. *Inorganic Chemistry Communications*, **148:** 110319 (2023).

[24] Parajuli, D. & Samatha, K. Topological properties of MXenes. In *MXenes and their Composites*. Elsevier (2022).

[25] Parinitha, M. & Venkateshulu, A. *Synthesis, Characterization and Transport Property of Pani – Calcium Titanate Composites*, **2** (1): 495–498 (2013).

[26] Pedersen, B. F.; Augdahl, E.; Sara, A. N.; Åkeson, Å.; Theorell, H. et al. Interpretation of Infrared Spectra of Solid Alkali Metal Oxalates, their Hydrates and Perhydrates. *Acta Chemica Scandinavica*, **21**: 801–811 (1967).

[27] Pilban, S.; Zak, A. K.; Majid, W. H. A. & Muhamad, M. R. Synthesis and Characterization of Lead Calcium Titanate Nanocomposite. *AIP Conference Proceedings*, **1328** (1): 183–185 (2011).

[28] Rai, A. K.; Rao, K. N.; Vinoth, L. K. & Mandal, K. D. Synthesis and characterization of ultra fine barium calcium titanate, barium strontium titanate and Ba1−2xCaxSrxTiO3 (x = 0.05, 0.10). *Journal of Alloys and Compounds*, **475** (1–2): 316–320 (2009).

[29] Shah, D. K.; K. C., D.; Parajuli, D.; Akhtar, M. S.; Kim, C. Y. & Yang, O. B. A computational study of carrier lifetime, doping concentration, and thickness of window layer for GaAs solar cell based on Al2O3 antireflection layer. *Solar Energy*, **234:** 330–337 (2022).

[30] Sharma, Y. K.; Kharkwal, M.; Uma, S. & Nagarajan, R. Synthesis and characterization of titanates of the formula MTiO3 (M = Mn, Fe, Co, Ni and Cd) by co-precipitation of mixed metal oxalates. *Polyhedron*, **28** (3): 579–585 (2009).

[31] Shimura, K.; Miyanaga, H. & Yoshida, H. Preparation of calcium titanate photocatalysts for hydrogen production. *Studies in Surface Science and Catalysis*, **175:** 85–92 (2010).

[32] Taïbi-Benziada, L.; Khereddine, Y.; Kerdja, T. & Henda, K. New Green Dielectrics Related to Calcium Titanate: Synthesis and Characterizations. *Arabian Journal for Science and Engineering*, **40** (10): 2873–2879 (2015).

[33] Tripathy, A.; Pramanik, S.; Manna, A.; Shah, N. F. A.; Shasmin, H. N. et al. Synthesis and Characterizations of Novel Ca-Mg-Ti-Fe-Oxides Based Ceramic Nanocrystals and Flexible Film of Polydimethylsiloxane Composite with Improved Mechanical and Dielectric Properties for Sensors. *Sensors*, **16** (3): 292 (2016).

[34] Wiff, J. P.; Fuenzalida, V. M.; Arias, J. L. & Fernandez, M. S. Hydrothermal–electrochemical CaTiO3 coatings as precursor of a biomimetic calcium phosphate layer. *Materials Letters*, **61** (13): 2739–2743 (2007).

[35] Zhao, H.; Duan, Y. & Sun, X. Synthesis and characterization of CaTiO3 particles with controlled shape and size. *New Journal of Chemistry*, **37** (4): 986–991 (2013).

[36] Zheng, H.; Bagshaw, H.; Csete de Györgyfalva, G. D. C.; Reaney, I. M.; Ubic, R. & Yarwood, J. Raman spectroscopy and microwave properties of CaTiO3-based ceramics. *Journal of Applied Physics*, **94** (5): 2948–2956 (2003).

[37] Zheng, H.; Reaney, I. M.; de Györgyfalva, G. D. C. C.; Ubic, R.; Yarwood, J. et al. Raman spectroscopy of CaTiO 3 -based perovskite solid solutions . *Journal of Materials Research*, **19** (2): 488–495 (2004).